Journal of Rock Mechanics and Geotechnical Engineering 13 (2021) 745–754

Contents lists available at ScienceDirect

Journal of Rock Mechanics and Geotechnical Engineering

journal homepage: www.jrmge.cn

Full Length Article

Performance of identical rockbolts tested on four dynamic testing rigs employing the direct impact method

Charlie C. Li [a,*], John Hadjigeorgiou [b], Peter Mikula [c], Greig Knox [d], Bradley Darlington [e], Renée Royer [f], Andrzej Pytlik [g], Michael Hosp [h]

[a] Norwegian University of Science and Technology (NTNU), Trondheim, Norway
[b] University of Toronto, Toronto, Canada
[c] Mikula Geotechnics Pty. Ltd., Kalgoorlie, Australia
[d] New Concept Mining, Johannesburg, South Africa
[e] Sandvik Mining & Rock Technology, Heatherbrae, Australia
[f] CanmetMINING, Natural Resources Canada, Ottawa, Canada
[g] Central Mining Institute, Katowice, Poland
[h] Minova, Innovation and Development Ground Support, Feistritz, Austria

ARTICLE INFO

Article history:
Received 24 September 2020
Received in revised form
16 November 2020
Accepted 21 January 2021
Available online 5 February 2021

Keywords:
Dynamic test
Drop test
Impact test
Rockbolt
Rock reinforcement
Ground support

ABSTRACT

Impact drop tests are routinely used to examine the dynamic performance of rockbolts. Numerous impact tests have been carried out in the past decades on independently designed, constructed and operated testing rigs. Each laboratory has developed testing procedures; thus, the results are often reported in different ways by various laboratories. The inconsistency in testing procedures and reporting formats presents a challenge when comparing results from different laboratories. A series of impact tests of identical rockbolts was carried out using the direct impact method (i.e. the mass free-fall method) on the rigs in four laboratories in different countries. The purpose of these tests was to investigate the level of consistency in the results from the four rigs. Each rig demonstrated a high level of repeatability, but differences existed between the various rigs. The differences would suggest that there is noticeable equipment-dependent bias when test results obtained from different laboratories are compared. It was also observed that the energy dissipated for the plastic displacement of the bolt was smaller than the impact energy in the tests. The average impact load (*AIL*) and the ultimate plastic displacement (*D*) of the bolt describe the ultimate dynamic performance of the bolt. In the case where the bolt does not rupture, the specific plastic energy (*SPE*) is an appropriate parameter in describing the impact performance of the bolt. Two other relevant parameters are the first peak load (*FPL*) and the initial stiffness (*K*) of the bolt sample. The information from this test series will guide the formulation of standardised testing procedures for dynamic impact tests of rockbolts.

1. Introduction

Rockbolts are an integral part of all ground support systems employed to mitigate the impact of a rockburst and other types of dynamic loading in underground hard rock excavation. In this context, rockbolts must be strong, yieldable and of high energy absorption when exposed to dynamic loading. The actual loading of a rockbolt during a rockburst event is a complicated process that cannot be fully captured during an impact test. Nevertheless, impact tests have some similarities to the loading process of rockbolts, for instance, during a strain burst event. Impact tests do provide useful information on the anticipated dynamic response of rockbolts under mining-induced seismic conditions. A large number of impact tests have been carried out on different types of rockbolts in the past decades in many countries including Canada, Australia, South Africa and China (Kaiser et al., 1995; Ortlepp et al., 2001; Simser, 2001; Gaudreau et al., 2004; Simser et al., 2006; Charette, 2007; Charette and Plouffe, 2007; Li, 2010; Wu and Oldsen, 2010; Galler et al., 2011; Cai and Champaigne, 2012; Li

* Corresponding author.
E-mail address: Charlie.c.li@ntnu.no (C.C. Li).
Peer review under responsibility of Institute of Rock and Soil Mechanics, Chinese Academy of Sciences.

https://doi.org/10.1016/j.jrmge.2021.01.003

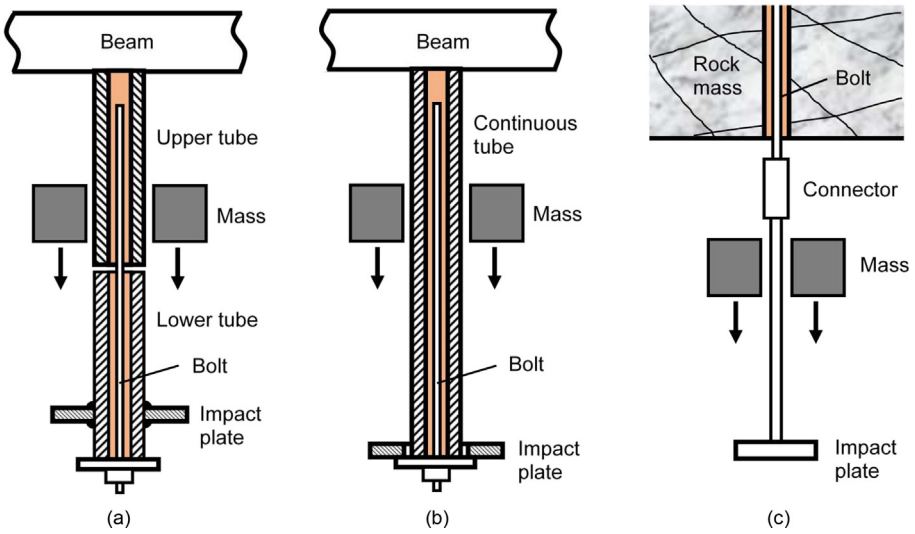

Fig. 1. Three types of arrangements for the direct impact method: (a) Use of a split-tube sample in the laboratory; (b) Use of a continuous tube sample in the laboratory (Li, 2017a, b); and (c) The test in the field (Darlington et al., 2018).

and Doucet, 2012; Player et al., 2013; Charette et al., 2014; He et al., 2014; He et al., 2017; Darlington et al., 2018; Berghorst and Knox, 2019; Sharifzadeh et al., 2020a, b). The tests were carried out on independently designed and constructed testing rigs in several laboratories. Each laboratory has developed testing procedures; therefore, test results are often reported in different ways. The absence of a standardised testing procedure and reporting format presents a challenge when comparing results between rigs. One issue with impact tests of rockbolts is that, although similar, none of the existing testing rigs are identical. Notable differences include the stiffness of the loading system, the sharpness of the impact, and the proportion of energy lost during the impact. These can contribute to a level of uncertainty in the interpretation of the testing results.

Before standardising the testing procedures, it is necessary to understand the differences between the test rigs and the effect on the result. This paper presents the results of a series of tests carried out on four testing rigs in different countries. All four testing rigs were independently designed and constructed by the operating laboratories. The technical specifications of the testing rigs vary, but all apply the impact load through the direct impact method. The main objective of the organised testing programme was to investigate whether consistent impact results could be obtained from tests of identical rockbolts on the four testing rigs. It is anticipated that the test results provide useful information that can contribute to standardising the testing procedure for the direct impact method and the reporting format of test results.

2. Direct impact method

Two methods are used to test the dynamic impact performance of rockbolts (Hadjigeorgiou and Potvin, 2011; Li, 2017a), i.e. the direct impact method (e.g. Kaiser et al., 1995; Knox et al., 2018; Simser, 2001) and the momentum transfer method (Villaescusa et al., 2013). It should be recognised that the accepted naming terminologies for the two test methods do not fully describe the loading process. For instance, momentum transfer is essentially involved in both test methods. In the direct impact method, a free-falling mass impacts with an impact plate attached to the sample, thereby applying a load. While in the momentum transfer method, both mass and bolt free-fall at the beginning of the test. The bolt is then abruptly stopped, and the momentum of the mass is transferred to the rockbolt. All four test rigs that were used for this investigation employed the direct impact method. The direct impact method has been used not only for laboratory tests but also for field tests (Darlington et al., 2018; Mikula and Brown, 2018).

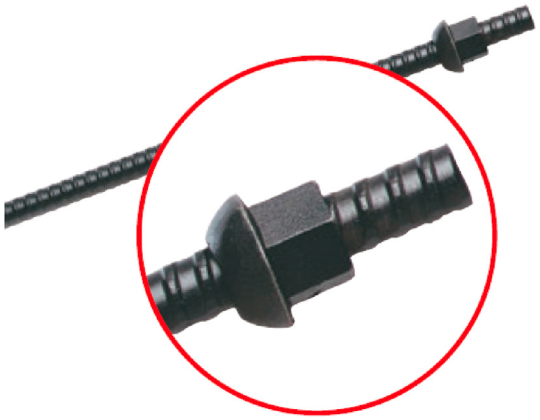

Fig. 2. The ϕ22 mm thread bar used in the tests (provided by the bolt supplier).

For laboratory tests, the bolt is installed in a split-tube (Fig. 1a) or a continuous tube (Fig. 1b). A split-tube configuration is used to simulate the loading condition of a bolt by an impact thrust ejection. The continuous tube configuration simulates the situation when the impact load is directly applied onto the bolt plate. The upper tube is suspended on the beam of the testing rig. A mass drops from a defined height onto the impact plate that is attached to the lower tube in the case of the split-tube sample or onto the impact plate attached directly to the bolt head in the case of the continuous tube sample. The position of impact plate on the split-tube sample is dependent on the design of the rockbolt. The bore of the steel tube is roughened to prevent slippage between the steel tube and the anchoring grout.

For the field tests by the direct impact method, the rockbolt is directly installed in the rock mass (Fig. 1c). An adapter is used to connect the bolt head to the loading assembly. The loading assembly is composed of a free-fall mass and a load-transferring rod. The advantage of the in situ direct impact method is that the rock

mass environment and the rockbolt installation practices are taken into account in the test; however, control over the parameters presents a challenge. The loading point at the bolt head is similar to that of a continuous tube loading in the laboratory.

3. Impact tests

For this investigation, several identical thread bar rockbolt specimens were sent to each of the laboratories. All tests were carried out according to an agreed testing specification. The intent of the tests was to test the consistency between the rigs rather than the performance of the rockbolts.

3.1. Bolt type

The bolts were a type of thread bar with a nominal diameter of ϕ22 mm (Fig. 2). According to the product specification of the bolt supplier, the bar was an ASTM (American Society for Testing and Materials) Grade 75 with a minimum yield load of 200 kN and a minimum ultimate load of 267 kN.

3.2. Testing specification

The performance of a rockbolt is a function of the mechanical properties, configuration, installation method and quality of the installation. Many factors influence the results of rockbolt tests. The encapsulation quality of fully grouted rockbolts is an example. If a rockbolt is fully encapsulated in a hole with resin cartridges, it would be difficult to guarantee that the encapsulation quality of the resin would be identical when installed in different laboratories. The purpose of the organised tests in this study was to examine the consistency of the test results between the four testing rigs, not the performance of the specific rockbolts. Therefore, it was decided that the bolts should not be encapsulated in holes but directly suspended at their upper ends to avoid bias caused by installation quality, thus removing a possible source of inconsistency between the testing rigs. One of the four rigs, Rig 1, is a testing facility in the field and its test arrangement is illustrated in Fig. 3a. On Rig 1, the bolt sample was installed in a ϕ28 mm borehole drilled in the rock mass. The upper 500 mm of the bolt was encapsulated in the borehole to form an anchor. The remaining length was stretched during impact. The other three rigs (Rigs 2–4) are laboratory testing facilities. The upper end of the bolt was suspended on the beam of the testing rig using a flat bearing plate and two nuts, as illustrated in Fig. 3b. It was required that all plates and nuts at the lower end of the bolt were not deformable preventing energy loss in the deformation of those elements. The mass was dropped from a given height H and impacted the plate at the lower end of the bolt. The impact caused elongation of the stretch length L of the bolt, which is defined as the axial displacement of the bolt.

The bolts delivered for testing were 1950 mm in length. It was specified that the stretch length L should be 1600 mm, the drop mass 2000 kg, and the drop height H 1000 mm. It was also recognised that each laboratory would modify the specified parameters to adapt to the limitations of its testing rig. For comparative purposes, the impact energy should be approximately 20 kJ for each drop.

Based on the collective experience from previous laboratory tests, it was recognised that the metal-to-metal impact often creates a frequency that could damage the load cell under the impact plate. Rubber-like pads were therefore positioned on the top of the impact plate to dampen the impact on the first three rigs. However, Rig 4 did not use damping pads so that the mass directly impacted onto the plate.

4. Test results

The impact tests were carried out in all four laboratories in accordance with the testing specification described in Section 3.2. All tests were undertaken under the direct supervision of the respective laboratories. In total eleven bolts were tested with two bolts on Rig 1, three on Rig 2, two on Rig 3, and four on Rig 4. The stretch length of the tested bolts was 1385 mm on Rig 1 and 1600 mm on Rigs 2–4. The drop mass was approximately 2000 kg

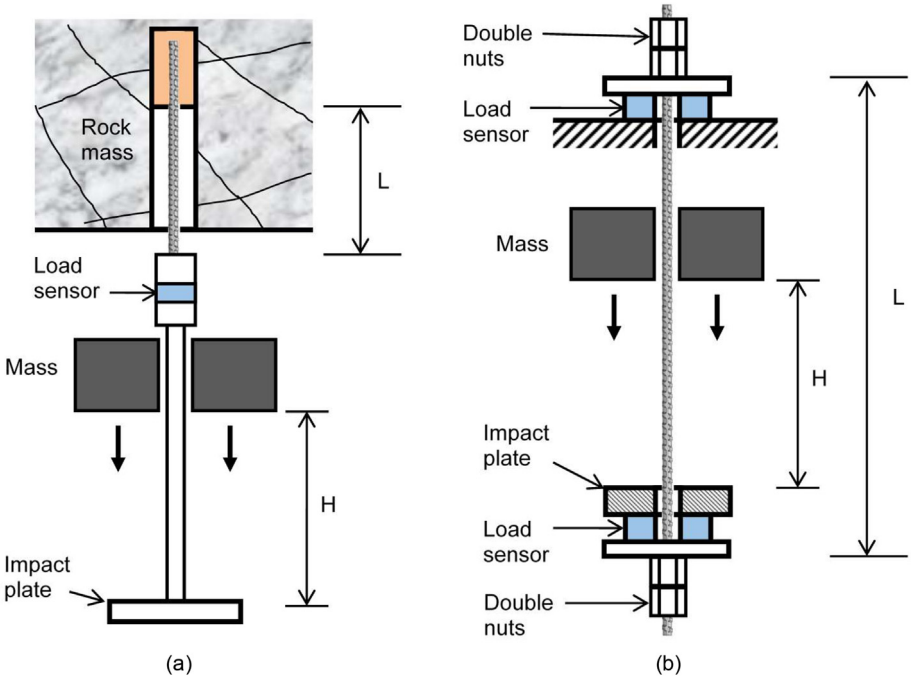

Fig. 3. Test arrangements of (a) Rig 1 in the field and (b) Rigs 2–4 in the laboratory.

and the drop height was 1000 mm, corresponding to approximately 20 kJ impact energy with an impact velocity of 4.4 m/s. The impact load was measured by a sensor placed at the lower end of the bolts on the first three rigs (also on the upper end on Rig 3) and the upper end on Rig 4. The effect of load sensor position is assessed in Section 6.4. The dimensions of the bolts and the testing input parameters on each testing rig are presented in Table 1.

Axial displacements were measured on the bolt plate at the lower end of the bolt. The axial displacement is approximately equal to the elongation of the stretch length of the bolt since the upper toe of the bolt had a minimal net movement. The test results are presented in diagrams of the impact load versus displacement in Fig. 4, the impact load versus time in Fig. 5 and the displacement versus time in Fig. 6. Each bolt sample is labelled by a testing facility number and a number for the bolt sample in Figs. 4–6 and in presentations below. For example, Rig 1-B1 refers to bolt sample B1 tested on testing facility Rig 1. It should be noted that the presented information is for the first impact and does not include the bounces after the impact and until the system returns to rest. The data presented are collected in the period from the initial loading to the time at which the impact load returns to zero owing to rebound. Data from the bounces are regarded as artefacts associated with the stiffness of both the bolt and the rig. Hence, the bounces do not affect the permanent energy dissipation capacity of the bolt and therefore are excluded from the reported results.

5. Analysis of test results

5.1. Comparison of the results

While only two to four bolts were tested on each rig, useful observations on similarities and differences between the rigs can still be made because of the repeatability of the results on each rig. It is seen in Figs. 4–6 that all response curves obtained on the same rig correlate, implying that the results are consistent on the same rig. The test results obtained on Rigs 1–3 are similar. However, the curves of the impact load versus displacement and versus time obtained on Rig 4 (Figs. 4d and 5d) appear different from those obtained on the other three rigs. The observed biases can be attributed to either the differences in the configuration of the testing rigs or the alignment of the bolt sample. Equally, it could be attributed to a combination of both.

The linear rising portion of the load–displacement curve in Fig. 4 represents the elastic response of the bolt to the impact load. The first peak load is a representative quantity for the yield load of the bolt. The plateau after the first peak load marks the stage during which the bolt deforms plastically. The load–displacement behaviour of the curves at the pre-peak stage is linear in Fig. 4a and d, but bilinear in Fig. 4b and c. The nearly vertical part of the bilinear segment might be caused by delayed responses of the displacement sensors or by effects of inertia on the two rigs.

Fig. 5 illustrates that the impact load rises linearly with time during the elastic deformation stage of the bolt. The total time from the beginning of the impact to the bounce onset varies from 50 ms to 59 ms between rigs. It should be noted that the stretch length of the bolts tested on Rig 1 (Fig. 5a) is slightly shorter (~13%) than those bolt samples tested on the other three rigs. Consequently, the impact-bounce onset time is shorter on Rig 1 than on the other rigs. Similarly, the displacement of the bolts on Rig 1 is slightly less than that reported in the other rigs.

Fig. 6 shows that the displacement of the bolt increases with time until the drop mass starts to rebound upwards. The ultimate displacement is reached at the end of the impact. After that, the mass tends to rebound upwards resulting in a decrease in the bolt load. The declining part of the displacement–time curve after the ultimate displacement marks the unloading. At the end of the unloading, the displacement decreases to the permanent quantity remaining beyond the elastic displacement.

The impact load fluctuated much more on Rig 4 than on the other rigs in the period when the bolt plastically deformed. The reasons for this fluctuation are not clear at this time. It was noted that Rig 4 used a type of strain-gauge sensor for load measurement, while the other three rigs used a type, or a similar type, of piezo-electric load sensor. The response of the strain-gauge sensor could be slower than the piezoelectric sensors, which might be one explanation for the load fluctuation. Furthermore, Rig 4 did not use damping pads on the impact plate as done by the other three rigs. It is not sure whether the impact without damping also contributed to the load fluctuation.

5.2. Characteristic parameters of impact tests

In this paper, a bolt sample refers to an installed rockbolt and is, therefore, either end anchored or fully grouted. Hence, a bolt sample is composed of a bolt and its anchoring means. Fig. 7 shows a typical load–displacement curve of a bolt sample subjected to an impulse. The load rises approximately linearly until the first peak load (*FPL*) is reached. The slope of the secant line from the origin to the point *FPL* is defined as the initial stiffness (*K*) of the bolt sample. The initial stiffness is dominated by the elasticity of the bolt sample but is also affected by the slight plasticity occurring before the first peak load. After the *FPL*, substantial plastic deformation occurs until the peak displacement of the drop mass is reached, and the mass starts to rebound upwards. Then, the load in the bolt sample linearly decreases to zero at which point the permanent plastic displacement (*D*) of the bolt sample is recorded. The shaded area under the curve represents the energy dissipated for the plastic deformation, which is called the plastic energy (*PE*) dissipation of the bolt sample. The ratio of *PE* to *D* is the average impact load (*AIL*), which also represents the energy dissipation of the bolt sample per unit plastic displacement, which is called the specific plastic energy (*SPE*) dissipation in this paper:

$$AIL = SPE = \frac{PE}{D} \tag{1}$$

It follows that the parameters *AIL* (or *SPE*), *D*, *FPL* and *K*

Table 1
Dimensions of the bolt samples and the testing parameters.

Testing Rig	Number of bolts	Bolt samples		Input parameters					Position of load sensor
		Bar diameter (mm)	Stretch length (mm)	Drop mass (kg)	Drop height (mm)	Impact velocity (m/s)	Impact energy (kJ)	Sampling frequency (kHz)	
Rig 1	2	22	1385	2068	985	4.4	20	25	At lower end
Rig 2	3	22	1600	2006	1020	4.47	20.1	10	At lower end
Rig 3	2	22	1600	2025	1000	4.43	19.9	10	At lower end
Rig 4	4	22	1600	1970	1000	4.43	19.3	19.2	At upper end

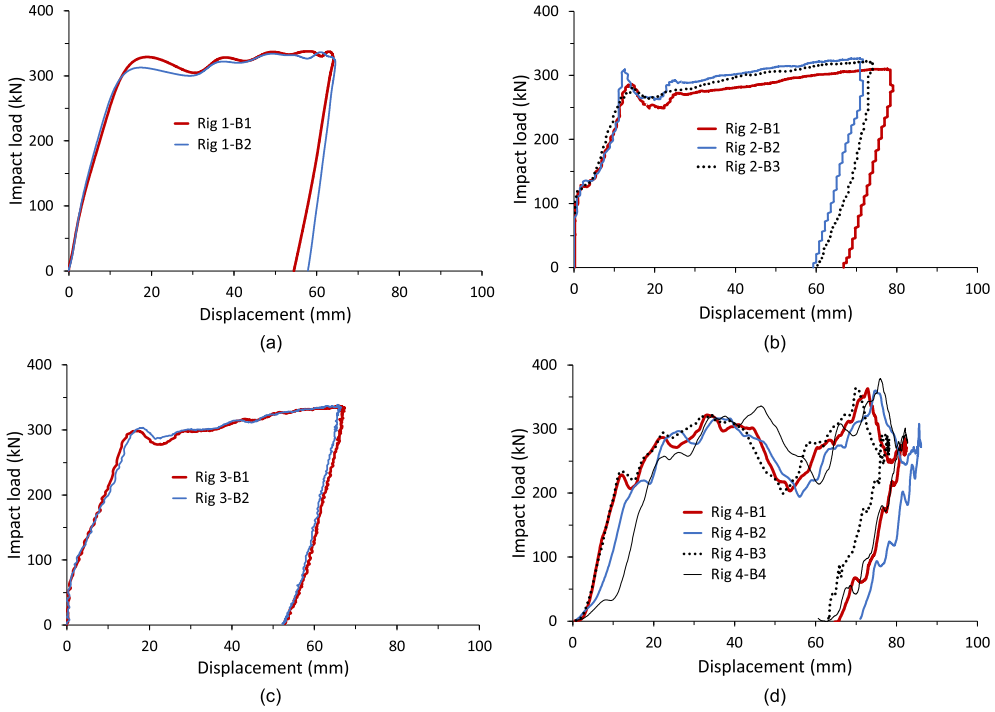

Fig. 4. The impact load versus displacement for the bolt samples tested on (a) Rig 1, (b) Rig 2, (c) Rig 3, and (d) Rig 4.

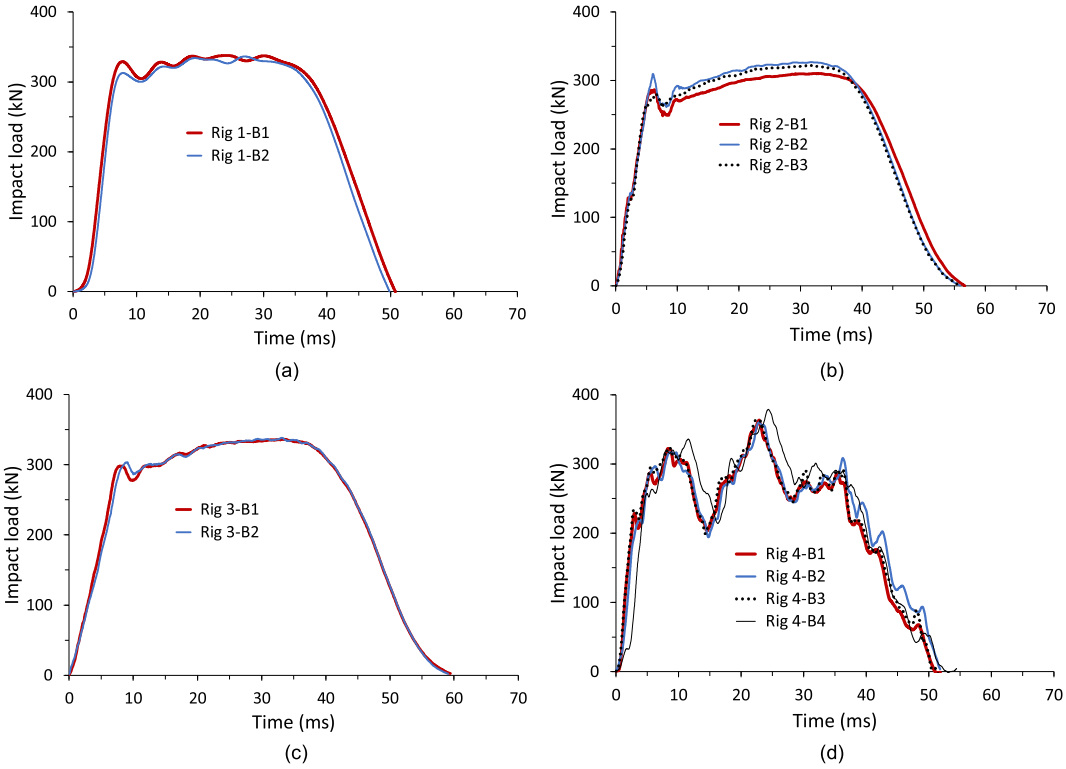

Fig. 5. The impact load versus time for the bolt samples tested on (a) Rig 1, (b) Rig 2, (c) Rig 3, and (d) Rig 4.

adequately describe the performance of a rockbolt sample that did not rupture under the impact load. However, two additional parameters, the ultimate energy dissipation and the ultimate displacement are required to fully illustrate the performance of a rockbolt that ruptures under the impact. These two parameters are outside the scope of this study and will not be discussed further.

The relevant characteristic parameters for the tested rockbolt samples were calculated from the load–displacement curves in

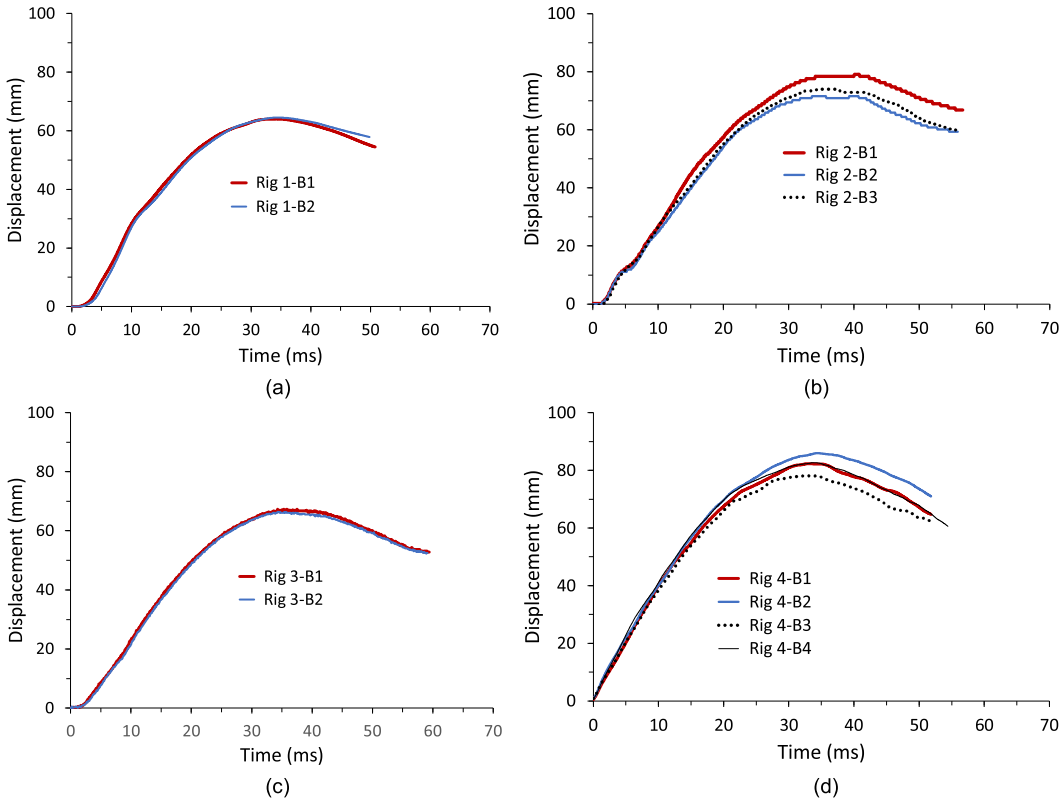

Fig. 6. The displacement versus time for the bolt samples tested on (a) Rig 1, (b) Rig 2, (c) Rig 3, and (d) Rig 4.

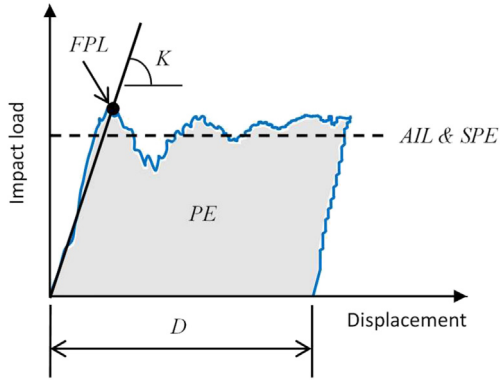

Fig. 7. A typical impact load–displacement curve of a rockbolt and the definitions of the plastic energy (*PE*) dissipation, the permanent plastic displacement (*D*), the average impact load (*AIL*), the specific plastic energy (*SPE*) dissipation, the first peak load (*FPL*), and the initial stiffness (*K*).

Fig. 4 and presented in Table 2. Numerically, the average impact load (*AIL*) and the specific plastic energy (*SPE*) are the same, but physically they have different meanings. Therefore, the names of both are listed in the same column in the table. The total energy input is calculated at the potential energy of the mass relative to its final position after the impact. Hence, it is the sum of the impact energy and extra energy input due to the permanent displacement *D* of the bolt. The impact energy is equal to the product of the mass, gravitational acceleration and the drop height. The extra energy input resulting from the change in length of the bolt is equal to the product of the mass, gravitational acceleration and the permanent displacement *D* after the impact. A small portion of the total energy input is lost in the forms of vibration, friction, sound and heat during impact so that the energy dissipated for plastic deformation of the rockbolt is smaller than the total energy input. The quantities of the lost energy are also presented in the table. The absolute lost energy is the difference between the total energy input and the plastic energy dissipated by the bolt. The lost energy in percentage is relative to the total energy input. The impact energy is 20 ± 0.1 kJ on Rigs 1–3 and 19.3 kJ on Rig 4. The extra energy input due to the permanent displacement *D* varies from 1 kJ to 1.4 kJ among the tested bolts. The lost energy is similar among the bolts tested on the same rig but varies substantially from 9% to 21% among the four rigs.

The plastic energy (*PE*) and the plastic displacement (*D*) of the rockbolt samples in Table 2 are obtained from the curves in Fig. 4. The average impact load (*AIL*), as well as the specific plastic energy (*SPE*), is calculated from the *PE* and *D* using Eq. (1). The *AIL* varies from 292 kN to 318 kN with a deviation of 26 kN among the seven bolts tested on the first three rigs. The *AIL* is lower on Rig 4 than on the other three rigs, ranging from 264 kN to 281 kN. The lower values of the *AIL* on Rig 4 could be due to the use of the low sensitivity strain-gauge load sensor. The first peak load *FPL* varies from 281 kN to 329 kN for the first three rigs, while it is in a range of lower values from 220 kN to 257 kN on Rig 4.

The initial stiffness (*K*) varies considerably between 11.4 MN/m and 22 MN/m among the tested bolt samples. Nevertheless, it is consistent among the bolt samples tested on the same rig among the first three rigs but less consistent on Rig 4. Based on the testing specification given in this study, the initial stiffness should be slightly less than the axial stiffness of the stretch segment of the bolt. As by definition, the slope of the secant line from the origin to the first peak load (*FPL*) includes a small portion of plastic deformation. However, the measured values of *K* are much less than the stiffness of the bolts which is in the range of 48–55 MN/m assuming that the Young's modulus of the steel is 200 GPa. The

Table 2
Summary of the results of the impact tests.

Rig No.	Bolt No.	Impact energy (kJ)	Extra input due to D (kJ)	Total energy input (kJ)	PE (kJ)	Total lost energy, W_{loss}[a]		D (mm)	AIL (kN)/SPE (J/mm)	FPL (kN)	K (MN/m)
						Value (kJ)	Percentage (%)[b]				
Rig 1	B1	20	1.1	21.1	17.3	3.8	18	54.5	318	329	17.5
	B2	20	1.2	21.2	17.7	3.5	16	57.9	306	313	18.1
Rig 2	B1	20.1	1.3	21.4	19.5	1.9	9	66.8	292	286	20.1
	B2	20.1	1.2	21.3	18.2	3.1	14	60.8	300	309	22
	B3	20.1	1.2	21.3	18.8	2.4	11	59.8	315	281	19.2
Rig 3	B1	19.9	1	20.9	16.7	4.2	20	52.8	317	298	17
	B2	19.9	1	20.9	16.5	4.4	21	52.5	314	304	16.5
Rig 4	B1	19.3	1.3	20.6	18.5	2.1	10	65.7	281	228	18.7
	B2	19.3	1.4	20.7	18.7	2	10	70.7	264	220	12.5
	B3	19.3	1.2	20.5	17.4	3.2	15	62.9	276	234	19.2
	B4	19.3	1.2	20.5	17.3	3.2	16	63	275	257	11.4

[a] Total lost energy W_{loss} = Total energy input − plastic energy PE.
[b] Percentage of total energy input (%).

initial stiffness (K) is affected by the fixture elements in the test arrangement, such as the load sensor, connecting adapters, nuts, and plates, and with the co-linearity of these elements. Consequently, it is more meaningful to compare the initial stiffness of different types of rockbolts tested on the same rig than tested on different testing rigs.

The permanent displacements of the bolts were also manually measured after testing. A deviation ranging between 0% and 20% was found when comparing instrument-measured (Table 2) and manually recorded displacements. Strict calibration of the measurement instruments is extremely important to obtain reliable test results.

6. Discussion

6.1. A conceptual model for the direct impact method

The energy transformation in the direct impact test can be explained with the help of the conceptual model illustrated in Fig. 8. The entire testing system can be simplified to two elements connected in series in the model: one for the testing rig and the other for the bolt sample to be tested. Each element consists of a spring to store the elastic energy and a frictional slider to dissipate the plastic energy. At the end of the impact, the average impact load (AIL) is the same both in the rockbolt and in the testing rig. The rockbolt stores elastic energy (W_{kb}) and dissipates plastic energy (PE) in the form of permanent deformation of the bolt. At the same time, the testing rig stores elastic energy (W_{km}) and dissipates energy (W_{pl}) through irreversible processes such as friction at the connecting joints of the test alignment. The elastic energies stored in the bolt and the testing rig are respectively written as

$$W_{kb} = \frac{1}{2K_b} AIL^2 \tag{2}$$

$$W_{km} = \frac{1}{2K_m} AIL^2 \tag{3}$$

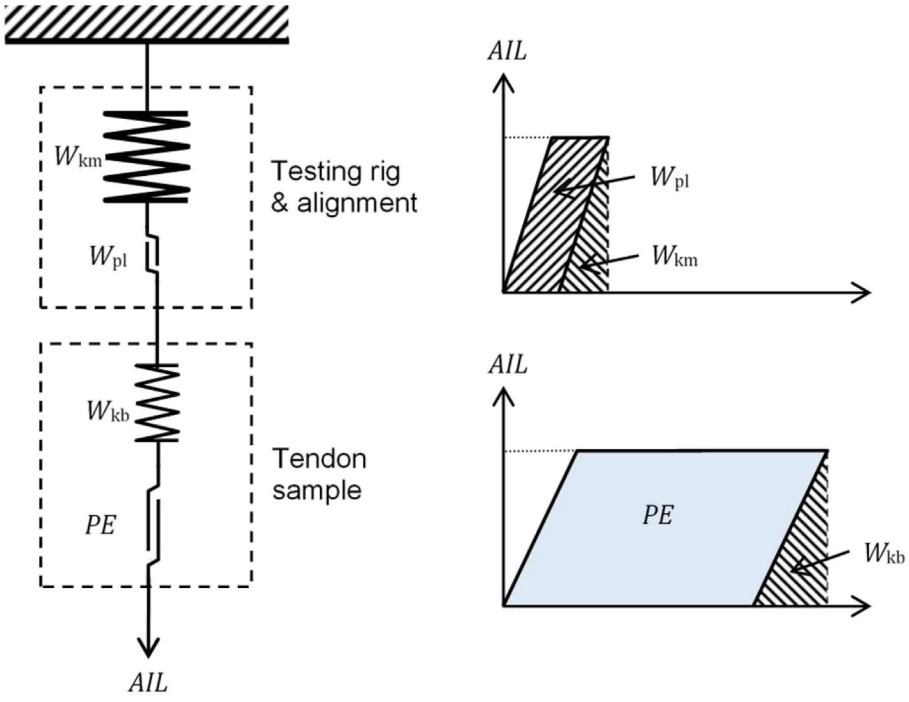

Fig. 8. A conceptual model for the testing rig by the direct impact method to illustrate the energy transformation during the test.

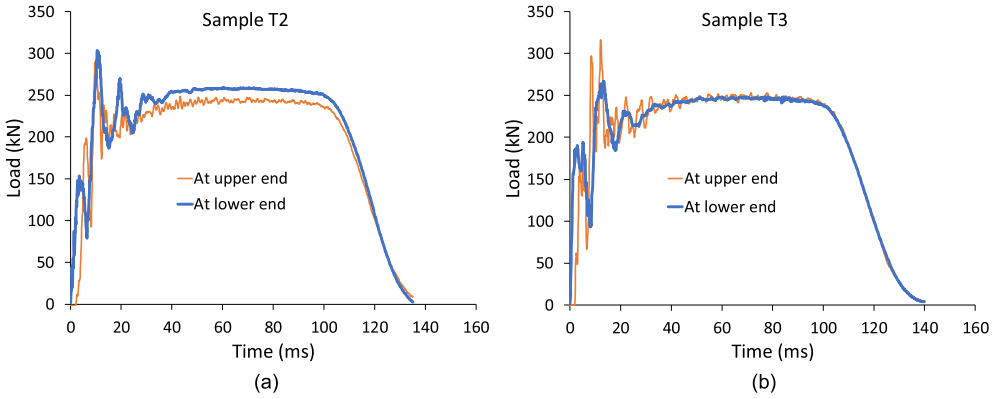

Fig. 9. The loads measured by sensors placed at the lower and upper ends of two bolt samples during dynamic impact tests: (a) Sample T2, and (b) Sample T3.

where K_b is the stiffness of the rockbolt and K_m is the stiffness of the testing rig. The elastic energies stored in the bolt and the testing rig will be released to rebound the mass at the end of the first impact. They are accounted as energy loss since they do not contribute to the plastic displacement of the bolt. The elastic energy will be transformed to heat and vibration during the subsequent bounces. Therefore, the total lost energy W_{loss} in the test is the sum of the three components W_{kb}, W_{km} and W_{pl}, i.e.

$$W_{loss} = W_{kb} + W_{km} + W_{pl} \quad (4)$$

Take the bolt samples in the tests as examples. The bolt diameter is ϕ22 mm, the stretch length of the bolt is 1.6 m and the average impact load *AIL* is approximately 300 kN. Assuming that the Young's modulus of the steel is 200 GPa, the stiffness of the stretch segment of the bolt, K_b, is 47.5 MN/m. The elastic energy stored in the bolt is obtained from Eq. (2) as $W_{kb} = 0.95$ kJ. It means that the elastic energy in the bolt is approximately one-third of the typical total lost energy. The frame stiffness of one of the testing rigs was determined as 121.3 MN/m. The elastic energy stored in the rig frame is obtained from Eq. (3) as $W_{km} = 0.37$ kJ. The sum of the elastic energy stored in the bolt and in the frame of the testing rig is 1.32 kJ which is approximately 40% of the typical total lost energy. The remaining 60% of the total lost energy was dissipated in the test alignment. The amount of the total elastic energy stored in the testing system is a constant for a specific bolt sample and testing rig. One way to reduce the energy loss is to reduce the number of connecting joints in the test alignment.

6.2. Field and laboratory tests

Rig 1 is a test facility in the field. The bolt to be tested is installed in a borehole drilled in the rock mass. Rig 1 essentially can be used to test rockbolts in underground operation so that it is a type of field dynamic test facility. The other three rigs are laboratory facilities. The outcomes of the tests, i.e. the values of *PE*, *D*, *AIL*, *FPL*, *K*, and the energy loss, both in the field and in the laboratories are similar. The consistent test results indicate that the testing conditions of the laboratory testing rigs are similar to the in situ testing condition of Rig 1, at least for the tested bolt configuration.

6.3. Total energy input and dissipated plastic energy

At present, the total energy input, the displacement *D* and the average impact load *AIL* are usually used to describe the dynamic performance of the rockbolt. As seen in the test results presented in Table 2, the energy dissipated for the plastic displacement of the bolt after the impact is smaller than the total energy input. The deviation varied from 9% to 21% among the rigs in the tests. The specific plastic energy *SPE* is a more appropriate parameter than the total energy input in describing the dynamic performance of a rockbolt for the case where the bolt does not rupture during the impact. Given that all rigs are independently designed and constructed, the energy loss could vary significantly if the sample alignment is not standardised.

6.4. Loads measured at the lower and upper ends of the rockbolt

It is a concern whether the loads measured at the lower and upper ends of the bolt are consistent. Additional impact tests were carried out on Rig 3 by placing load sensors both at the lower and upper ends of the samples, as shown in Fig. 3b. In this series of tests, the drop mass was 3216 kg and the drop height was 1.5 m, corresponding to 47.3 kJ impact energy and 5.4 m/s impact velocity, respectively. Fig. 9 shows the measured loads versus the time for two of the tube samples. There is a good agreement between the loads measured at the lower and upper ends of the tube samples. The drop mass hit the impact plate so that the load sensor at the lower end recorded the impact before the sensor at the upper end. The time offset between the two sensors was 2.3 ms for sample T2 and 2 ms for T3. The average load was slightly higher at the lower end than at the upper end. For sample T2, the average load was 210 kN at the lower end and 197 kN at the upper end. For sample T3, it is 196 kN at the lower end and 194 kN at the upper end. In conclusion, the difference in the loads measured at the lower and upper ends of the samples is low. It is preferable that the load sensor should be placed underneath the impact plate at the lower end of the sample, given this is where the average load is the highest. Nevertheless, it is acceptable that the load sensor is placed at the upper end of the sample.

6.5. On the bounces after the first impact

It has been a concern whether the bounces after the first impact contribute to plastic deformations in the rockbolt. Knox and Berghorst (2018) observed in their tests that the ultimate loads in the subsequent bounces never exceeded the yield load of the bolt. Fig. 10 shows the impact and the subsequent bounces of bolt Rig 2-B1. The ultimate loads of the bounces were always lower than the yield load of the bolt shank. Hence, the bounces do not cause any further plastic displacement in the bolt. The load–displacement

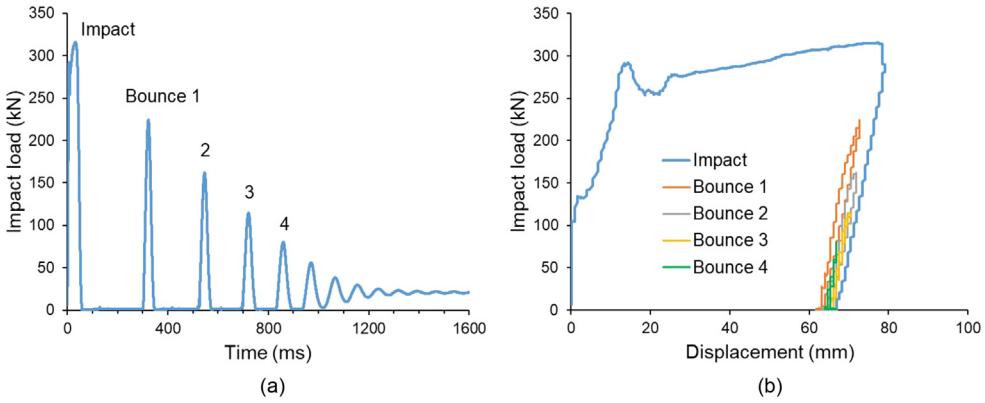

Fig. 10. The first impact and the elastic bounces of bolt Rig 2-B1 as a function of (a) time and (b) displacement.

hysteresis loops during the bounces indicate that the elastic bounce energy was transformed to heat during the bounces.

7. Conclusions

This investigation provided a unique opportunity to explore the consistency of results obtained by four independently operating rigs in North America, Australia, Europe and Africa. In a specifically designed series of tests, a high level of repeatability between the test results was observed on the same rig. Nevertheless, there are measurable differences in the results obtained from the different testing rigs. Therefore, there may be noticeable equipment-dependent bias in the test results. These results are the first step towards developing a calibrating process that will allow greater confidence when comparing the results from different laboratories.

A portion of the energy input is lost in the forms of vibration and friction during the impact. The specific plastic energy dissipated while displacing the bolt is a more appropriate parameter than the total energy input in describing the dynamic performance of the rockbolt that does not rupture after the impact. An amount of energy is lost during bouncing of the drop mass, the vibration of the rig frame and test elements, and friction in the connecting joints of the test alignment.

In addition to the ultimate energy absorption and the ultimate displacement, the specific plastic energy (*SPE*), the first peak load (*FPL*) and the initial stiffness of the bolt sample (*K*) are also characteristic parameters in describing the dynamic performance of the rockbolt. As an important input parameter, the impact velocity, or the drop height, must be presented in the test report.

The impact load measured at the upper end of the bolt sample is slightly smaller than the load measured under the impact plate at the lower end. The difference is small so that both methods are acceptable for load measurement. However, the load measurement under the impact plate at the lower end of the bolt is preferred.

Overall, this study has demonstrated that although test results can be consistent on the same testing rig, they can vary between rigs. This information will guide the formulation of a standardised testing procedure for impact tests of rockbolts using the direct impact method.

Declaration of competing interest

The authors declare that they have no known competing financial interests or personal relationships that could have appeared to influence the work reported in this paper.

Acknowledgments

The authors are grateful to Devan MacDonald and Ted Anderson in Specialized Ground Control and Rock Mechanics Testing Laboratory, Canada, for their assistance in some of the laboratory tests.

Symbols and abbreviations

AIL	Average impact load of the bolt sample during the impact
D	Permanent plastic displacement of the bolt sample after the impact test
FPL	First peak load on the impact load–displacement curve or impact load-time curve
H	Drop height of the mass
K	Initial stiffness of the bolt sample, calculated on the impact load–displacement curve
K_b	Elastic stiffness of the stretch segment of the bolt sample
K_m	Elastic stiffness of the testing rig
L	Stretch length of the bolt sample
PE	Plastic energy dissipated for the permanent displacement *D* of the bolt sample after the impact test
SPE	Specific plastic energy that refers to the plastic energy dissipated for a unit permanent displacement of the bolt sample after the impact test
W_{kb}	Elastic energy stored in the bolt sample at the end of the impact
W_{km}	Elastic energy stored in the testing system at the end of the impact
W_{loss}	Total lost energy, equal to the sum of W_{kb}, W_{km} and W_{pl}
W_{pl}	Plastic energy dissipated in the testing rig and the test alignment

References

Berghorst, A., Knox, G., 2019. Introduction and application of the dynamic impact tester. In: Proceedings of the 53rd US rock mechanics/geomechanics symposium. American Rock Mechanics Association (ARMA), New York, NY, USA.

Cai, M., Champaigne, D., 2012. Influence of bolt-grout bonding on MCB conebolt performance. Int. J. Rock Mech. Min. Sci. 49, 165–175.

Charette, F., Hyett, A.J., Voyzelle, B., Anderson, T., 2014. Load-deformation behaviour of a deformable rockbolt and accessories under dynamic loading. In: Deep mining 2014. Australian Centre for Geomechanics, pp. 253–262.

Charette, F., Plouffe, M., 2007. Roofex – results of laboratory testing of a new concept of yieldable tendon. In: Deep mining 07 – proceeding of the 4th international seminar on deep and high stress mining. Australian Centre for Geomechanics, pp. 395–404.

Charette, F., 2007. Performance of Swellex rockbolts under dynamic loading conditions. In: Challenges in deep and high stress mining. Australian Centre for Geomechanics, pp. 387–392.

Darlington, B., Rataj, M., Balog, G., Barnett, D., 2018. Development of the MDX bolt and in-situ dynamic testing at telfer Gold mine. In: Rock dynamics – experiments, theories and applications. CRC Press, pp. 403–408.
Galler, R., Gschwandtner, G.G., Doucet, C., 2011. Roofex bolt and its application in tunnelling by dealing with high stress ground conditions. In: ITA-AITES world tunnel congress, Helsinki, Finland.
Gaudreau, D., Aubertin, M., Simon, R., 2004. Performance assessment of tendon support systems submitted to dynamic loading. In: Proceedings of the 5th international symposium on ground support. Taylor & Francis, pp. 299–312.
Hadjigeorgiou, J., Potvin, Y., 2011. A critical assessment of dynamic rock reinforcement and support testing facilities. Rock Mech. Rock Eng. 44, 565–578.
He, M., Gong, W., Wang, J., Qi, P., Tao, Z., Du, S., Peng, Y., 2014. Development of a novel energy-absorbing bolt with extraordinarily large elongation and constant resistance. Int. J. Rock Mech. Min. Sci. 67, 29–42.
He, M., Li, C., Gong, W., Sousa, L.R., Li, S., 2017. Dynamic tests for a constant-resistance-large-deformation bolt using a modified SHTB system. Tunn. Undergr. Space Technol. 64, 103–116.
Kaiser, P.K., McCreath, D.R., Tannant, D.D., 1995. Rockburst support. In: Canadian Rockburst Research Program 1990–1995 – A comprehensive summary of five years of collaborative research on rockbursting in hard rock mines, vol. 2. CAMIRO Mining Division.
Knox, G., Berghorst, A., Crompton, B., 2018. The relationship between the magnitude of impact velocity per impulse and cumulative absorbed energy capacity of a rock bolt. In: AusRock 2018 – the 4th Australian ground control in mining conference, pp. 160–169. Sydney, NSW, Australia. pp. 160–169.
Knox, G., Berghorst, A., 2018. Increased agility for the research and development of dynamic roof support products. In: Rock dynamics – experiments, theories and applications. CRC Press, pp. 373–384.
Li, C.C., Doucet, C., 2012. Performance of D-bolts under dynamic loading conditions. Rock Mech. Rock Eng. 45 (2), 193–204.
Li, C.C., 2010. A new energy-absorbing bolt for rock support in high stress rock masses. Int. J. Rock Mech. Min. Sci. 47 (3), 396–404.
Li, C.C., 2017a. Chapter 11: energy-absorbing rockbolts. In: Rock mechanics and engineering. Volume 4: excavation, support and monitoring. CRC Press, pp. 311–336.
Li, C.C., 2017b. Rockbolting: principles and applications. Butterworth-Heinemann.
Mikula, P.A., Brown, B.M., 2018. The need for additional dynamic testing methods for ground support elements. In: Rock dynamics – experiments, theories and applications. CRC Press, pp. 425–432.
Ortlepp, W.D., Bornman, J.J., Erasmus, N., 2001. The Durabar – a yieldable support tendon – design rationale and laboratory results. In: Rockbursts and seismicity in mines - RaSiM5. J. S. Afr. Inst. Min. Metall, pp. 263–264.
Player, J.R., Villaescusa, E., Thompson, A.G., 2013. Dynamic testing of fully encapsulated threaded bar – resin and cement grouted. In: Ground support 2013. Australian Centre for Geomechanics, pp. 247–264.
Sharifzadeh, M., Lou, J., Crompton, B., 2020a. Dynamic performance of energy-absorbing rockbolts based on laboratory test results. Part I: evolution, deformation mechanisms, dynamic performance and classification. Tunn. Undergr. Space Technol. 105, 103510.
Sharifzadeh, M., Lou, J., Crompton, B., 2020b. Dynamic performance of energy-absorbing rockbolts based on laboratory test results. Part II: role of inherent features on dynamic performance of rockbolts. Tunn. Undergr. Space Technol. 105, 103555.
Simser, B., Andrieux, P., Langevin, F., Parrott, T., Turcotte, P., 2006. Field behaviour and failure modes of modified conebolts at the Craig, LaRonde and Brunswick Mines in Canada. In: Deep and high stress mining.
Simser, B., 2001. Geotechnical review of the july 29th, 2001. West ore zone mass blast and the performance of the brunswick/NTC rockburst support system. Technical Report.
Villaescusa, E., Thompson, A.G., Player, J., 2013. A decade of ground support research at the WA School of Mines. In: Proceedings of the 7th international symposium on ground support in mining and underground construction. Australian Centre for Geomechanics, pp. 233–245.
Wu, Y.K., Oldsen, J., 2010. Development of a new yielding rock bolt – yield-Lok bolt. In: Proceedings of the 44th US rock mechanics symposium. ARMA.

Charlie Chunlin Li is a professor of rock mechanics for civil and mining engineering in the Norwegian University of Science and Technology (NTNU) in Norway. Before his academic career at NTNU, he worked as a research associate and an associate professor in Lulea University of Technology, Sweden; a ground control engineer in Boliden Mineral Ltd., Sweden; and the chief technical officer in Dynamic Rock Support AS, Norway. His expertise is in stability analyses of underground spaces and ground control. He is a member of the Norwegian Academy of Technological Sciences (NTVA). He was the International Society for Rock Mechanics and Rock Engineering (ISRM) Vice-President for Europe 2015–2019.

Peter Mikula graduated from the University of New South Wales in Sydney, Australia in 1980. He worked for ACIRL Ltd. and Coffey Partners International. From 1993, he spent 12 years at Mt Charlotte Gold Mine, Kalgoorlie, becoming familiar with practical issues including seismicity and underground stope stability. He was also a key player in mine safety, accident investigation, and risk management.

Bradley Darlington is an R&D design Engineer at Sandvik Mining and Rock Technology. He completed his Bachelor of Engineering (Mechanical) in 2009 and has worked in Sandvik's Bolting division since 2011. Over this time, he has been involved with the design and implementation of new products into Sandvik's ground support product offering. He has also managed the design, development, introduction and continued application of the first ever in situ Dynamic Test Rig.

Renée Royer works as a ground control engineer at CanmetMINING beginning in 2015 to present. She has worked in the mining industry for 15 years in various roles as geologist, ground control engineer, underground mining supervisor and mining development coordinator. She obtained her engineering degree in geology (BEng) at l'Université du Québec à Chicoutimi in 2001. She obtained her Master degree in Project Management (MPM) from l'Université du Québec en Outaouais in 2018.